

Micelles and Vesicles Formed by Polyoxometalate–Block Copolymer Composites**

Weifeng Bu, Sayaka Uchida, and Noritaka Mizuno*

Polyoxometalates (POMs) are anionic metal oxide clusters with several to a few tens of negative charges, and their structural and electronic versatility has resulted in various applications in the fields of catalysis, biomedicine, and materials science.^[1] However, these hydrophilic clusters are basically incompatible with hydrophobic organic materials and have high lattice energies associated with crystallization. Therefore, further fabrication of POM-based materials and devices requires manipulating the clusters on the nanoscale through solution-based self-assembly.

The surface properties of POMs can be modified by replacement of the counteranions with cationic surfactants to form surfactant-encapsulated clusters (SECs).^[2] The resultant SECs are soluble in organic media and facilitate fabrication of POM-based thin films such as Langmuir monolayers, Langmuir–Blodgett films, and solvent-cast films. On the other hand, ionic block copolymers are macromolecular analogues of conventional ionic surfactants. They can self-assemble into regular and reverse micellelike nanosized aggregates in aqueous media and nonpolar organic solvents, respectively.^[3] The morphologies of the aggregates primarily depend on the incompatibility between blocks, block compositions, and solvents.

Poly(styrene-*b*-4-vinyl-*N*-methylpyridinium iodide), S_n - b - V_m , with long *S* and short *V* blocks can form multiple morphologies of aggregates (i.e., sphere, cylinder, and bilayer) on dispersion in water.^[4] However, only reverse spherical micelles have been reported for this block ionomer family in toluene.^[5] Combination of S_n - b - V_m with oppositely charged block ionomers leads to formation of asymmetric vesicles.^[6] Here we report the preparation of POM/block copolymer composites and their self-assembly into micelles and vesicles in organic solvents. The micelles reach the

superstrong segregation (SSS) regime, where the ionic core radii correspond to the length of fully stretched *V* blocks, the interface is totally occupied by *S*/*V* junction points, and no more space is available to incorporate chains.^[7]

The POM/ S_n - b - V_m (SVP) composites (Figure 1) were prepared by electrostatic incorporation of POMs into solid S_n - b - V_m matrices as follows: $\text{Na}_3[\alpha\text{-PW}_{12}\text{O}_{40}]$ was dissolved in water and the pH value modified to 0.7–0.8 with aqueous

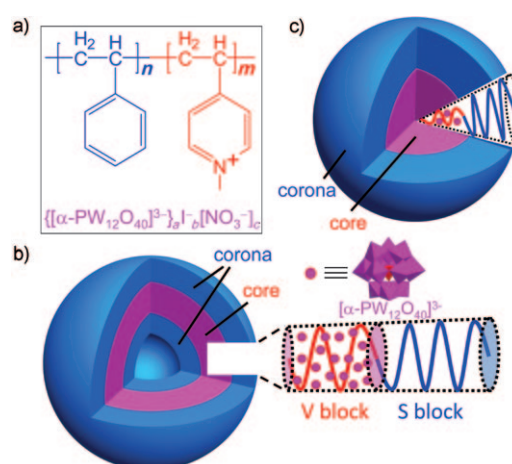


Figure 1. a) Structural formulas and schematic drawings of POM/ S_n - b - V_m (SVP) composites with b) vesicular and c) micellar morphology.

HNO_3 .^[8] This solution was added to a suspension of S_n - b - V_m powder ($n = 240$, $m = 65$; $n = 480$, $m = 57$; and $n = 1171$, $m = 206$) in water. The resultant mixture was vigorously stirred for 3 d and the solid product collected (SVP-1 to SVP-7). The IR spectra of the composites showed the characteristic bands of both $[\alpha\text{-PW}_{12}\text{O}_{40}]^{3-}$ and block ionomers.^[9] The compositions of SVP-1–SVP-7 and parameters such as the weight fractions of POM (W_{POM}) and hydrophilic volumes (V_h) are listed in Table 1.

Since the *S* blocks are soluble in toluene and the *V* blocks in combination with POM are insoluble in toluene, the self-assembled morphologies of these composites in toluene were studied with transmission electron microscopy (TEM). A typical TEM image of SVP-1 showed vesicular aggregates in a quasi-hexagonal array (Figure 2a). The vesicular nature is evidenced by the higher transmission in the center (b) than around the periphery (a) of the dark capsules. The TEM image did not show any significant difference on the rotation of the sample with respect to the electron beam at angles of -30 to $+30^\circ$, that is, the vesicles are spherical (Figure S1, Supporting Information). Energy-dispersive X-ray (EDX)

[*] Dr. W. Bu, Dr. S. Uchida, Prof. Dr. N. Mizuno
Department of Applied Chemistry, School of Engineering
The University of Tokyo, Hongo, Bunkyo-ku, Tokyo 113-8656 (Japan)
Fax: (+81) 3-5841-7220
E-mail: tmizuno@mail.ecc.u-tokyo.ac.jp

[**] W.B. is grateful for a JSPS Fellowship. This work was supported by the Core Research for Evolutional Science and Technology (CREST) program of Japan Science and Technology Agency (JST), and Grants-in-Aid for Scientific Research, Center for Nano Lithography and Analysis, and The University of Tokyo Global COE Program Chemistry through Cooperation of Science and Engineering from the Ministry of Education, Culture, Sports, Science, and Technology (MEXT) of Japan. Drs. H. S. Kato (RIKEN) and S. Inasawa (Univ. of Tokyo) are acknowledged for the SFM measurements. Rigaku corporation is acknowledged for the SAXS and XRF measurements.

Supporting information for this article is available on the WWW under <http://dx.doi.org/10.1002/anie.200904116>.

Table 1: Molecular and packing characteristics of S_n - b - $V_m/[\{\alpha\text{-PW}_{12}\text{O}_{40}\}^3]_a[\text{NO}_3^-]_b$ formed in 1 mg mL^{-1} toluene dispersions.

| Sample | n | m | a | b | c | $W_{\text{POM}}^{[a]}$ | V_h [nm ³] ^[b] | D_v [nm] ^[c] | D_s [nm] ^[d] | R_0 [nm] ^[e] | A_c [nm ²] ^[f] | $N_{\text{agg}}^{[g]}$ | $S_c^{[h]}$ | $N_v^{[i]}$ |
|--------|------|-----|-----|-----|-----|------------------------|---|---------------------------|---------------------------|---------------------------|---|------------------------|-------------|-------------------|
| SVP-1 | 240 | 65 | 17 | 14 | 0 | 0.58 | 25.9 | 10 (v) | 7 | 12 | 5.3 | 2.6×10^3 | 0.31 | 4.4×10^4 |
| SVP-2 | 1171 | 206 | 46 | 28 | 40 | 0.46 | 77.8 | 19 (v) | 14 | 30 | 8.4 | 6.9×10^3 | 0.18 | 3.2×10^5 |
| SVP-3 | 480 | 57 | 18 | 3 | 0 | 0.49 | 24.6 | 8 (v) | 10 | 18 | 6.3 | 9.6×10^2 | 0.28 | 1.7×10^4 |
| SVP-4 | 480 | 57 | 16 | 7 | 2 | 0.44 | 23.1 | 10 (v) | 13 | 18 | 4.8 | 2.2×10^3 | 0.35 | 3.5×10^4 |
| SVP-5 | 480 | 57 | 12 | 4 | 17 | 0.37 | 20.9 | 32 (m) | 13 | 18 | 3.9 | 8.2×10^2 | 1.12 | 9.8×10^3 |
| SVP-6 | 480 | 57 | 8 | 1 | 32 | 0.28 | 18.8 | 12 (v) | 13 | 18 | 3.9 | 1.4×10^3 | 0.42 | 1.6×10^4 |
| SVP-7 | 480 | 57 | 5 | 1 | 41 | 0.19 | 16.5 | 32 (m) | 12 | 18 | 3.1 | 1.0×10^3 | 1.12 | 5.2×10^3 |

[a] Weight fraction of POM. [b] Hydrophilic volume per formula (including iodide, nitrate, POMs, and V blocks). [c] Core diameter of micelles (m) and wall thickness of vesicles (v). [d] Corona thickness. [e] Unperturbed end-to-end distance of the S block. $R_0 = 0.456 n^{0.595}$.^[13] [f] Interfacial area per chain. [g] Calculated by dividing the volume of the core by V_h . [h] Ratio of the core radius (micelles) or wall thickness (vesicles) to the contour length of V blocks ($m \times 0.25\text{ nm}$). [i] Average number of POMs per aggregate estimated from N_{agg} and the composition of SVP composites. Details of the calculations of packing parameters are given in the Supporting Information.

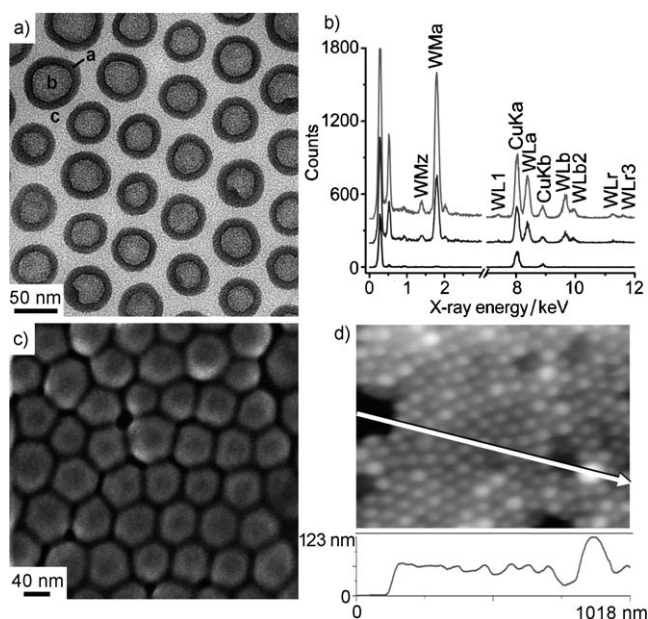


Figure 2. a) TEM image of SVP-1. b) EDX spectra of a–c (top to bottom). c) SEM image and d) SFM sectional analysis of SVP-1. The samples from 1 mg mL^{-1} toluene dispersion were drop-cast on carbon-coated copper grids for microscopic observations.

measurements (Figure 2b) showed that tungsten is present in both **a** and **b**, while no tungsten was detected in the in-between area (**c**). The tungsten concentration in **a** is higher than that in **b**. Therefore, **a** corresponds to the vesicle core filled with POMs bound to V blocks by Coulomb forces. The average diameter of the dark capsule and wall thickness are $(56 \pm 10)\text{ nm}$ and $(10 \pm 0.9)\text{ nm}$, respectively. The corona contains the S blocks and was not observed by TEM due to the low electron density of the corona compared with the core. The average distance between vesicles was $(70 \pm 26)\text{ nm}$.

The surface morphology of SVP-1 was observed by means of scanning electron microscopy (SEM) and scanning force microscopy (SFM) images (Figure 2c and d). Both SEM and SFM images revealed quasihexagonal arrays of spherical aggregates. Both the average diameter $((71 \pm 21)\text{ nm})$ and height $((70 \pm 5)\text{ nm})$ of the aggregates agreed fairly well with the average intervesicle distance observed in the TEM image,

that is, the overall diameter of the vesicle is about 70 nm. The corona thickness of the vesicle was estimated to be 7 nm by subtraction of the diameter of the dark capsule (ca. 56 nm) from that of the vesicle (ca. 70 nm).

Incorporation of POMs into S_{1171} - b - V_{206} and S_{480} - b - V_{57} formed SVP-2 and SVP-3, respectively, with spherical vesicular aggregates in quasihexagonal arrays (Figure 3a and Figure S2, Supporting Information). Block ionomers with long hydrophobic blocks and short hydrophilic blocks form spherical micelles in hydrophobic organic solvents.^[5,10] In contrast, incorporation of large amounts of POMs into S_n - b -

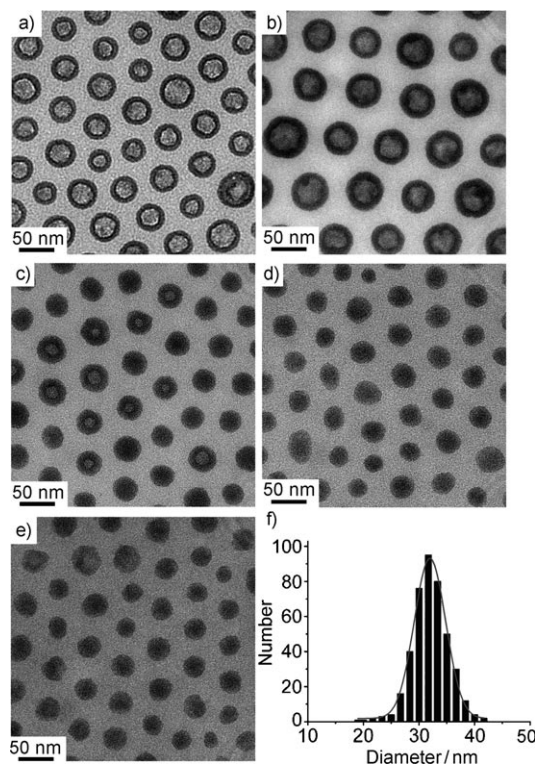


Figure 3. TEM images of a) SVP-3, b) SVP-4, c) SVP-5, d) SVP-6, and e) SVP-7 drop-cast from 1 mg mL^{-1} toluene dispersion. f) Core-diameter distribution of the spherical micelles of SVP-7. The solid line represents the Gaussian fit, and the average diameter is $(32 \pm 5.7)\text{ nm}$ ($R^2 = 0.99$).

V_m led to the formation of vesicles in toluene. This sharp contrast raises the question of the formation mechanism of SVP vesicles. To answer this question, the number of POM units with respect to the block ionomer were controlled by using a block ionomer $S_{480}-b-V_{57}$ with the largest hydrophobic-to-hydrophilic ratio (SVP-3–SVP-7).

The TEM image of SVP-4 showed vesicles in quasihexagonal arrays (Figure 3b). Both vesicles and spherical micelles in quasihexagonal arrays were observed with decreasing amounts of POMs (SVP-5, Figure 3c). Spherical micelles in quasihexagonal arrays were observed with further decreases in the amounts of POM [SVP-6 (Figure 3d) and SVP-7 (Figure 3e)]. The EDX measurements showed that tungsten and iodine are present in the dark spheres and absent in the in-between areas. Therefore, the dark spheres corresponding to the micellar core contain POMs, iodide, and nitrate bound to V blocks by Coulomb forces. The average core and overall micelle diameters for SVP-7 are (32 ± 5.7) and (55 ± 7.2) nm, respectively (Figure 3f). Small-angle X-ray scattering (SAXS) studies reflect the structures of the core due to its higher electron density compared to the corona. The SAXS pattern of SVP-7 in toluene (Figure 4a) could be

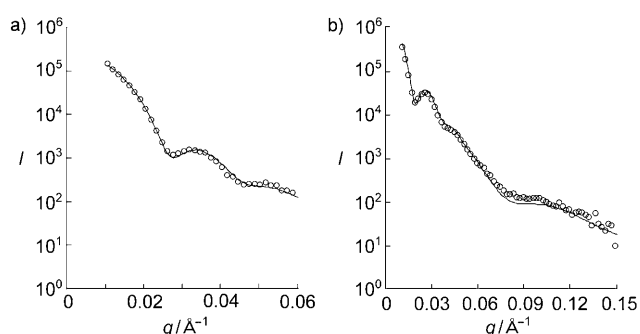


Figure 4. SAXS patterns of a) SVP-7 and b) SVP-3 in toluene (ca. 0.3 mg L^{-1}). The open circles indicate the experimental data. The solid line in a) shows the pattern calculated for a micelle with a core diameter of (34 ± 3.6) nm. The solid line in (b) shows the pattern calculated for a vesicle with an outer core diameter of (39 ± 5.0) nm and a wall thickness of (7.9 ± 1.6) nm.

reproduced with a micellar model, and the calculated core diameter $((34 \pm 3.6) \text{ nm})$ agreed fairly well with that obtained from the TEM image $((32 \pm 5.7) \text{ nm})$. The SAXS pattern of SVP-3 in toluene (Figure 4b) could be reproduced with a vesicle model, and the calculated outer core diameter $((39 \pm 5.0) \text{ nm})$ and wall thickness $((7.9 \pm 1.6) \text{ nm})$ were in fair agreement with those obtained from the TEM image $((38 \pm 7.1) \text{ nm}$ and $(8.0 \pm 0.7) \text{ nm}$, respectively).^[11] These results show that there is no significant difference in the morphologies of SVP composites in the film (TEM, SEM, and SFM) and solution (SAXS) states, and that the aggregates of SVP composites are stable on evaporation of toluene.

The core radii of the micelles in SVP-5–SVP-7 (16 nm) agreed fairly well with the length of the fully stretched (contour length) V_{57} block (14.25 nm). Therefore, the micelles

reached the SSS regime, as theoretically suggested by Khoklov et al. (vide infra).^[7] The SSS regime can be reached if 1) the interfacial tension between insoluble blocks and solvents/soluble blocks is rather high, 2) attraction between insoluble blocks is very strong, and 3) the length of insoluble blocks is relatively small.^[5,7,13] The SAXS studies by Eisenberg et al. showed that the ionic core radii of reverse micelles of S_n-b-V_m with long V blocks ($m \geq 30$) are shorter than the contour lengths of the V blocks, because the entropy is decreased by stretching the long V blocks. On the other hand, the micelles in the SSS regime were directly observed by TEM for SVP composites. This is probably due to the increase in the interfacial tension between the ionic species and toluene/S blocks on incorporation of hydrophilic POMs. An intermediate state with both micelles and vesicles (SVP-5) was observed with increasing W_{POM} , and on further increasing W_{POM} only vesicles formed (SVP-4 and SVP-3). The wall thicknesses of the vesicles of SVP-5, SVP-4, and SVP-3 were 12, 10, and 8 nm, respectively, and they decreased with increasing W_{POM} . The changes in the morphologies of the composites are probably explained as follows: While an increase in W_{POM} leads to increases in hydrophilic volume and interfacial tension, further expansion of the micelles in the SSS regime is impossible, and the morphology changes from micellar to vesicular. The wall thickness of the vesicles (i.e., length of the V block) decreases with increasing W_{POM} to compensate the increase in interfacial tension.

On the basis of the incompatibility of S blocks with the ionic cores and sharp interface between the core and corona in the TEM images, it is probable that the core is free of S blocks and toluene. Therefore, packing parameters such as the interfacial area per chain (A_c), chain stretching degree (S_c) for V blocks, and aggregation number (N_{agg}) were calculated to characterize the micellar and vesicular structures quantitatively (Table 1).^[3–5] The N_{agg} values of the SVP composites were much larger than those of the parent S_n-b-V_m , and this suggests that the interfacial tensions are high. The S_c values of the vesicles (0.18–0.42) were smaller than those of the micelles (1.12), while the A_c values of the vesicles (3.9 – 8.4 nm^2) were larger than those of the micelles (3.1 – 3.9 nm^2). These results could be explained by the larger W_{POM} values of the vesicles (0.37–0.58) compared to the micelles (0.19–0.37), and thus the higher interfacial tensions of the vesicles. To compensate the larger interfacial tensions, the entropy is increased by shrinking the V blocks, which causes a decrease in S_c followed by an increase in A_c . In the case of SVP-3–SVP-5 vesicles, S_c decreased from 0.42 to 0.28, while A_c increased from 3.9 to 6.3 nm^2 , with increasing W_{POM} , which could be explained in the same way.

In summary, incorporation of $[\alpha\text{-PW}_{12}\text{O}_{40}]^{3-}$ into S_n-b-V_m matrices leads to the formation of composites with micellar and vesicular morphologies. The self-assembled morphologies and sizes of the composites in toluene are primarily governed by the following factors: 1) increased hydrophilic volume fraction and 2) interfacial tension between the ionic species and the toluene/S blocks. The present concept of combining POM chemistry with solution self-assembly of block copolymers will open a new avenue to developing POM-based functional materials and devices.

Experimental Section

Materials and instruments: Poly(styrene-*b*-4-vinyl-*N*-pyridinium-methyl iodide), S_n -*b*- V_m , was purchased from Polymer Source Inc. and used without further purification. The subscripts denote the degrees of polymerization. The compositions were confirmed by the ratio between the integrated intensities of the ^1H NMR signals of styrene and pyridinium residues. $\text{Na}_3[\alpha\text{-PW}_{12}\text{O}_{40}]$ was obtained from Wako and used as received. Infrared (IR) spectra (KBr) were measured with a JASCO FT/IR-460 Plus spectrometer. ^1H NMR spectra were measured in $[\text{D}_7]\text{DMF}$ solutions on a JEOL JNM-EX-270 spectrometer (270 MHz). Residual protons of $[\text{D}_6]\text{DMF}$ were used as internal standard for the measurements. The TEM images were obtained with on a JEOL 2010HC instrument operating at 200 kV. The SEM images were obtained with a Hitachi S-4800. To prevent electric charging, a 2 nm-thick platinum layer was deposited on the specimen with a Hitachi E-1030 ion sputterer. The SFM images were obtained with a JEOL JSPM-4200 in tapping mode by using a silicon oxide cantilever. The SAXS measurements were performed with Rigaku Nano-Viewer with $\text{Cu}_{\text{K}\alpha}$ radiation (40 kV, 20 mA). Elemental analyses were performed with a Yanaco CHN Corder MT-6 (C, H, and N) and Rigaku energy-dispersive X-ray fluorescence (XRF) spectrometer EDXL 3000 (I, P, and W).

Preparation and characterization of SVP composites: SVP-1 was prepared as follows: $\text{Na}_3[\alpha\text{-PW}_{12}\text{O}_{40}]$ (300 mg, 0.102 mmol) was dissolved in water (20 mL) and the pH value was adjusted to 0.7–0.8 with aqueous HNO_3 . This solution was added to a suspension of S_{240} -*b*- V_{65} (86 mg, 2.10 μmol) in 10 mL of water with vigorous stirring. The resultant suspension was stirred for 3 d, whereby ion exchange of I^- with $[\alpha\text{-PW}_{12}\text{O}_{40}]^{3-}$ and NO_3^- took place. The solid product was collected by filtration, washed with water, and dried in vacuo (SVP-1). SVP-1 was dispersed in toluene (1 mg mL^{-1}), and the toluene solution was drop-cast on a carbon-coated copper grid for microscopy studies (TEM, SEM, and SFM). The morphologies of the aggregates of SVP composites observed by microscopy did not depend on the concentration of the toluene solution of SVP composites (0.3–1.0 mg mL^{-1}). The SAXS patterns of the 0.3 and 1.0 mg mL^{-1} toluene solutions were similar to each other, while the intensity of the latter was low because of the relatively large X-ray absorption. Therefore, the SAXS measurements and calculations were carried out with the 0.3 mg mL^{-1} toluene solutions. SVP-2 and SVP-3 were prepared according to the procedure for SVP-1 with S_{1171} -*b*- V_{206} and S_{480} -*b*- V_{57} , respectively. SVP-4, SVP-5, SVP-6, and SVP-7 were prepared according to the procedure for SVP-1, with molar ratios between S_{480} -*b*- V_{57} and $[\alpha\text{-PW}_{12}\text{O}_{40}]^{3-}$ in the synthetic solution of 1:16, 1:12, 1:8, and 1:5, respectively. The band positions of the IR spectra and elemental analyses are shown in the Supporting Information.

Received: July 24, 2009

Published online: September 24, 2009

Keywords: block copolymers · micelles · polyoxometalates · self-assembly · vesicles

- [1] a) M. T. Pope, *Heteropoly and Isopoly Oxometalates*, Springer, Berlin, **1983**; b) T. Okuhara, N. Mizuno, M. Misono, *Adv. Catal.* **1996**, *41*, 113; c) C. L. Hill, *Chem. Rev.* **1998**, *98*, 1; d) R. Neumann, *Prog. Inorg. Chem.* **1998**, *47*, 317; e) N. Mizuno, K. Yamaguchi, K. Kamata, *Coord. Chem. Rev.* **2005**, *249*, 1944; f) N. Casañ-Pastor, P. Gómez-Romero, *Front. Biosci.* **2004**, *9*, 1759; g) E. Cadot, M. J. Pouet, C. R. Labarre, C. du Peloux, J. Marrot, F. Sécheresse, *J. Am. Chem. Soc.* **2004**, *126*, 9127; h) A. Proust, R. Thouvenot, P. Gouzerh, *Chem. Commun.* **2008**, 1837; i) J. Zhang, Y. F. Song, L. Cronin, T. Liu, *J. Am. Chem. Soc.* **2008**, *130*, 14408.
- [2] a) D. G. Kurth, P. Lehmann, D. Volkmer, H. Cölfen, M. J. Koop, A. Müller, A. Du Chesne, *Chem. Eur. J.* **2000**, *6*, 385; b) D. Volkmer, A. Du Chesne, D. G. Kurth, H. Schnablegger, P. Lehmann, M. J. Koop, A. Müller, *J. Am. Chem. Soc.* **2000**, *122*, 1995; c) W. Bu, H. Li, H. Sun, S. Yin, L. Wu, *J. Am. Chem. Soc.* **2005**, *127*, 8016; d) H. Li, H. Sun, W. Qi, M. Xu, L. Wu, *Angew. Chem.* **2007**, *119*, 1322; *Angew. Chem. Int. Ed.* **2007**, *46*, 1300; e) D. Fan, X. Jia, P. Tang, J. Hao, T. Liu, *Angew. Chem.* **2007**, *119*, 3406; *Angew. Chem. Int. Ed.* **2007**, *46*, 3342; f) W. Bu, L. Wu, X. Zhang, A.-C. Tang, *J. Phys. Chem. B* **2003**, *107*, 13425; g) T. R. Zhang, C. Spitz, M. Antonietti, C. F. J. Faul, *Chem. Eur. J.* **2005**, *11*, 1001; h) X. Lin, Y. Wang, L. Wu, *Lamguir* **2009**, *25*, 6081.
- [3] a) M. Moffitt, K. Khougaz, A. Eisenberg, *Acc. Chem. Res.* **1996**, *29*, 95; b) S. Förster, V. Abetz, A. H. E. Müller, *Adv. Polym. Sci.* **2004**, *166*, 173.
- [4] a) Y. Yu, A. Eisenberg, *J. Am. Chem. Soc.* **1997**, *119*, 8383; b) Z. Gao, S. K. Varshney, S. Wong, A. Eisenberg, *Macromolecules* **1994**, *27*, 7923.
- [5] a) J. P. Gouin, C. E. Williams, A. Eisenberg, *Macromolecules* **1989**, *22*, 4573; b) J. P. Gouin, F. Bosse, D. Nguyen, C. E. Williams, A. Eisenberg, *Macromolecules* **1993**, *26*, 7250; c) D. Nguyen, X.-F. Zhong, C. E. Williams, A. Eisenberg, *Macromolecules* **1994**, *27*, 5173.
- [6] S. Schrage, R. Sigel, H. Schlaad, *Macromolecules* **2003**, *36*, 1417.
- [7] I. A. Nyrkova, A. R. Khokhlov, M. Doi, *Macromolecules* **1993**, *26*, 3601.
- [8] Nitrate is incorporated into S_n -*b*- V_m matrices besides POMs on syntheses in aqueous HNO_3 . The effects of nitrates on the morphologies of SVP composites were investigated by preparing a sample (SVP-7') according to the same method as that of SVP-7 except that aqueous HI was used instead of aqueous HNO_3 . The elemental analysis of SVP-7' suggested that more than 180 iodide/iodine with respect to S_{480} -*b*- V_{57} existed in the composite. While the TEM image of SVP-7 showed micelles in the SSS regime (Figure 3e), that of SVP-7' showed vesicles and micelles. The formation of vesicles in SVP-7' is probably explained as follows: While the existence of large amounts of iodide/iodine in the core increases the hydrophilic volume of SVP-7', further expansion of the micelles in the SSS regime is impossible and vesicles are formed.
- [9] In addition, characteristic IR bands of nitrate ($\nu_s(\text{NO}_3)$, 1384 cm^{-1}) were observed for the SVP composites.
- [10] The TEM images of S_n -*b*- V_m cast from toluene showed spherical micellar morphologies.
- [11] The major difference in the SAXS pattern between monodispersed micelles and vesicles was that the vesicle pattern contained a low-frequency oscillation corresponding to the wall thickness as well as a high-frequency oscillation corresponding to the outer core diameter (i.e., vesicular size), while the micelle pattern contained only the high-frequency oscillation.^[12] The SAXS pattern of SVP-3 in toluene contained both low- ($q = 0.09\text{--}0.15 \text{ \AA}^{-1}$) and high-frequency oscillations ($q = 0.02\text{--}0.07 \text{ \AA}^{-1}$), and could not be reproduced with the micellar model. Details of the SAXS calculations are given in the Supporting Information.
- [12] a) O. Glatter, O. Kratky, *Small Angle X-ray Scattering*, Academic Press, London, **1982**; b) G. Battaglia, A. J. Ryan, *Nat. Mater.* **2005**, *4*, 869; c) J. Bang, S. Jain, Z. Li, T. Lodge, J. S. Pedersen, E. Kesselman, Y. Talmon, *Macromolecules* **2006**, *39*, 1199.
- [13] S. Förster, M. Zisenis, E. Wenz, M. Antonietti, *J. Chem. Phys.* **1996**, *104*, 9956.